Check for updates

Toxic effects of zinc oxide nanoparticles combined with vitamin C and casein phosphopeptides on gastric epithelium cells and the intestinal absorption of mice†

Tianjiao Gu,[a] Chenjie Yao,[a] Kangkang Zhang,[a] Chenchen Li,[a] Lin Ding,[a] Yanan Huang,[a] Minghong Wu[*b] and Yanli Wang [ID] [*a]

Zinc oxide nanomaterials have become common food additives in recent years. Casein phosphopeptides (CPP) and vitamin C (VC) are used as functional food additives together with ZnO nanoparticles (ZnO NPs) in many commercial foods. Our previous studies showed that VC can increase the cytotoxicity induced by ZnO NPs both *in vitro* and *in vivo*, while CPP can have a cytoprotective effect against oxidative stress induced by ZnO NPs. However, the combined toxic effect of the three additives together in food is unknown. Herein, we have investigated the combined toxicity of ZnO NPs, CPP and VC by altering the sequence of their addition to clarify their toxic mechanisms in the composite systems. When the order of addition of the three materials changes, the cytotoxicity induced by the ZnO NPs changes due to the different concentrations of dissolved Zn ions in the different groups. We have also probed the intestinal absorption of Zn ions with an everted gut sac model. The amount of Zn^{2+} absorbed in the intestine in different composite systems also responds differently to the sequence of addition of the additives. VC is more powerful at controlling the synergistic toxic effect induced by ZnO NPs compared to the protective role of CPP in the combined systems.

Introduction

Engineered nanomaterials have been widely and increasingly used in the food industry in recent years. They are often used in food packaging, storage life sensors, food additives and juice clarifiers.[1] Due to the unique physicochemical properties of nanoparticles, such as their small size, high reactivity and good antibiotic properties, ZnO nanoparticles (ZnO NPs) are commonly used in food additives. ZnO NPs have also been used as a dietary supplement instead of zinc salts in human and livestock[2] because there are hundreds of functional enzymes containing Zn in the body[3] and zinc is an essential trace element for human body growth and brain promotion. Supplying Zn can also decrease the occurrence of contagious diseases.[4] The dramatic expansion of ZnO NPs in food has increased the amount of safety information on the food products in nanotechnology for the food sectors,[5] and it is necessary to investigate the potential toxic effects of ZnO NPs on human health.[6] The safety of ZnO NPs is related to its physicochemical

nature and the possible modes of exposure.[7] The toxicity of the single nano-ZnO has been commonly studied, and the standards for the safety evaluation of nano-ZnO additives in food mostly remain to be directed toward the single materials in simple food systems.[8] However, several additives with different functions are usually used together in one kind of food, but there are only a few reports about the combined biological effects of ZnO NPs with other materials in a complex system. Cao *et al.* found that palmitic acid (PA) could increase the production of mitochondrial reactive oxygen species (mROS) of Caco-2 cells to enhance the cytotoxicity induced by ZnO NPs, whereas free fatty acids (FFA) did not affect ROS production.[9] Li *et al.* reported that there was a positive correlation between the increase in concentration and the single toxicity of propiconazole and ZnO NPs to the NIH/3T3 cells, but the cytotoxicity decreased when the two compounds existed together.[10] In the food safety field, there have been several studies about the combined toxicity of ZnO NPs and other food additives.

Caseinophosphopeptides (CPP) are casein fragments that carry some phosphorylated serine residues.[11] CPP have both primary and secondary antioxidant abilities such as directly scavenging free radicals and isolating potential metal pro-oxidants.[12] Ascorbic acid, also known as vitamin C (VC), a water-soluble vitamin that can enhance human immunity and health, is effective at scavenging free radicals including hydroxyl

[a]Institute of Nanochemistry and Nanobiology, Shanghai University, Shanghai, China. E-mail: wangyanli@staff.shu.edu.cn

[b]School of Environmental and Chemical Engineering, Shanghai University, Shanghai, China. E-mail: mhwu@shu.edu.cn

radicals, aqueous peroxyl radicals and superoxide anions.[13] Therefore, VC often acts as a potent water-soluble antioxidant in biological fluids. We conducted a survey on the commercially available foods in the supermarket and based on our market survey results, we confirmed that ZnO NPs, CPP and VC are often included as food additives in the same foodstuffs. Our previous studies reported that VC significantly increased the toxicity of ZnO NPs both *in vitro* and *in vivo*.[8] CPP can protect GES-1 cells against injury induced by ZnO NPs by decreasing reactive oxygen species, diminishing the level of malondialde-hyde, increasing the content of glutathione and improving the activity of superoxide dismutase.[14] However, when ZnO NPs meet CPP and VC, one can protect GES-1 cells induced by ZnO NPs and the other can present synergistic toxicity with ZnO NPs in GES-1 cells. The combined toxic effect of the three additives remains unknown.

Herein, we further studied the combined toxic effect of ZnO NPs, CPP and VC by changing the sequence of addition, using a gastric epithelial cell line (GES-1) as the cellular model. Moreover, intestinal absorption is viewed as one of the critical factors for combined toxicity evaluation.[15] Seal *et al.* demon-strated that the colon has considerable capacity to absorb Zn ions by Na^{+}, K^{+}-ATPase-dependent mechanisms and that this capacity could be promoted by the consumption of pectin.[16] It was not known whether CPP and VC would influence Zn ion absorption in the small intestines of mice. To learn more about this, we used the everted gut sacs model to research Zn ion absorption, dissolved from ZnO NPs in the presence of CPP and VC, for the first time. The results demonstrate that CPP weakly protects from the toxic effect induced by ZnO NPs accompanied by VC. However, VC can still increase the toxicity induced by ZnO NPs even when all three of them co-exist in the composite system. The cytotoxicity resulting from changing the order of addition of ZnO NPs, CPP and VC varies due to the variation in the amount of Zn ions dissolved from ZnO NPs, which further confirms that the amount of dissolved Zn ions plays a key role in the toxicity of ZnO NPs in both the simple and composite systems.

Results and discussion

Characterization of ZnO NPs

The size of the nanoparticles is one of the main factors that have an effect on the engineering of the nanomaterials' functional-ities.[17,18] The size of NPs is able to powerfully affect their inter-actions with living cells, including the cytotoxicity.[19] The morphology and size of ZnO NPs were investigated by trans-mission electron microscopy (TEM). The shape and size of the ZnO NPs are shown in Fig. 1a, most of which are spherical or virgate. When ZnO NPs and CPP were combined, they generated serious aggregation (Fig. 1b). The dispersions of the ZnO plus VC, and ZnO NPs plus CPP plus VC groups were much better than the ZnO plus CPP group (Fig. 1c and d). Fig. 1e shows the X-ray (XRD) spectrum of the ZnO NPs. The diffraction peaks of ZnO NPs correspond to the hexagonal wurtzite structure of ZnO, which is in perfect accordance with the standard JCPDS file of ZnO (JCPDS card no. 36-1451). The size distribution of ZnO NPs
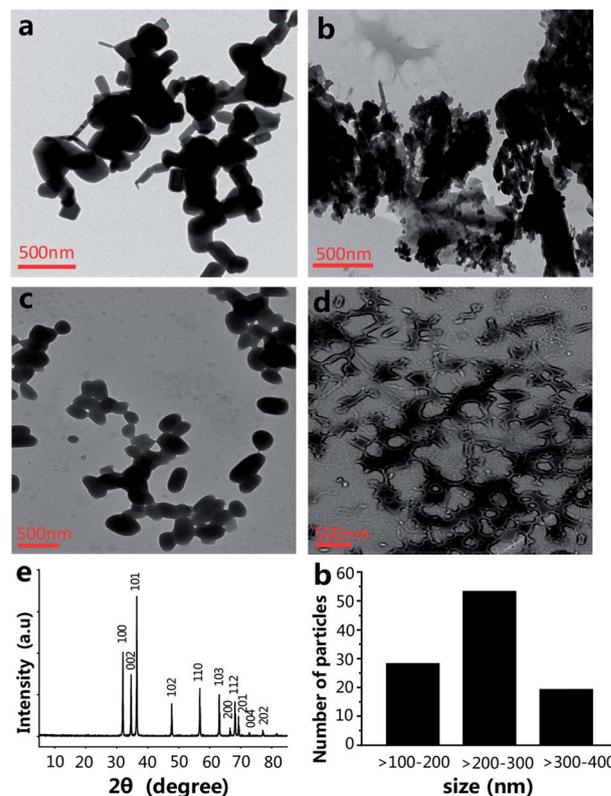

Fig. 1 Characterization of ZnO NPs, ZnO NPs plus CPP, ZnO NPs plus VC, ZnO NPs plus CPP plus VC: (a) TEM image of ZnO NPs; (b) TEM image of ZnO NPs plus CPP; (c) TEM image of ZnO NPs plus VC; (d) TEM image of ZnO NPs plus CPP plus VC; (e) XRD patterns of ZnO NPs were recorded in the range of 5–85 of 2 angles. All diffraction peaks can be perfectly indexed to hexagonal wurtzite structure of ZnO (JCPDS card no. 36-1451); (f) The size distribution of ZnO NPs.

is shown in Fig. 1f in TEM photos by counting approximately 100 particles using a Nano Measurer. The ZnO NPs sizes ranged from one hundred to four hundred nanometers, indicating the uneven size distribution of commercial food grade ZnO NPs. Dynamic light scattering (DLS) is a common method for measuring the hydrodynamic diameters and zeta potentials of the nanomaterials. From Table 1, DLS measurements indicate that the absolute values of the zeta potentials of ZnO NPs from four different composite systems in the medium are all lower than those in water. The hydrodynamic sizes of ZnO NPs in the medium are also larger than those in water. In particular, the

Table 1 Hydrodynamic diameter and zeta potential of ZnO NPs in combined systems[b]

	Particle size (nm)		Zeta potential (mV)	
	In water	In medium[a]	In water	In medium[a]
ZnO	157 ± 27	172 ± 13	−15.3 ± 0.9	−6.1 ± 0.2
ZnO + CPP	289 ± 16	357 ± 36	−13.3 ± 0.6	−7.5 ± 0.6
ZnO + VC	162 ± 29	194 ± 78	−11.3 ± 0.2	−6.7 ± 0.3
ZnO + CPP + VC	203 ± 68	276 ± 42	−14.0 ± 0.4	−9.7 ± 0.5

[a] Culture medium is high-glucose DMEM with 10% fetal bovine serum. [b] Data are presented as the mean ± S.D.

hydrodynamic size of ZnO NPs in the ZnO plus CPP group is up to 289 ± 29 nm in water and 357 ± 36 nm in the medium, with a hydrodynamic size that is the largest among the four groups, indicating that there is significant aggregation of ZnO NPs in the presence of CPP. The changes in the hydrodynamic sizes and the zeta potentials of ZnO NPs with the four complex groups in water and in the medium indicate that the stabilities of the four groups are not very good and they agglomerate more easily in the medium than in water.

Combined cytotoxicity study of ZnO NPs with CPP and VC

ZnO NPs, CPP and VC have generally been used in food additives. It has been verified that CPP has a cytoprotective effect on GES-1 cells against toxicity, while VC increases the toxicity induced by ZnO NPs in GES-1 cells. It is very important to know the combined effect of ZnO NPs in the presence of CPP and VC on GES-1 cells. To compare the cell viability of the GES-1 cells after co-incubation with different groups of the three materials, cell count, cell viability and LDH release were employed. The cell viability of GES-1 cells treated by the three single food additives and ZnO NPs plus CPP and ZnO NPs plus VC was once again confirmed.

Fig. S1a and c† show that there was no toxicity to the GES-1 cells, and cell viability was greater than 100% at the concentration of 10 or 15 mg L^{-1} of ZnO NPs and at the concentrations of VC that are less than 300 mg L^{-1}; it shows that 300 mg L^{-1} VC causes no injury to GES-1 cells. However, when 300 mg L^{-1} VC plus different concentrations of ZnO NPs were incubated with GES-1 cells, the cell viabilities decreased to about 80%, 50%, 19%, 17%, 15% in GES-1 (Fig. 2a). The cytotoxicity induced by ZnO NPs and VC was significantly increased, compared with the ZnO NPs alone, when 300 mg L^{-1} of VC was mixed with ZnO NPs. The viabilities of the cells exposed to different concentrations of CPP from 5 to 1000 mg L^{-1} were all nearly higher than 100%; i.e., CPP alone has no cytotoxicity toward GES-1 cells (Fig. S1b†). Additionally, when cells were treated with 500 mg L^{-1} of CPP plus different concentrations of ZnO NPs, the cell viabilities were all higher than the control group, which indicates that CPP prevents the damage to cells caused by ZnO NPs (Fig. 2b); these results are in accordance with our previous reports.[8,14] We therefore continued to use 15 mg L^{-1} ZnO NPs, 500 mg L^{-1} CPP and 300 mg L^{-1} VC as the final concentrations of the composite groups for the further study of the combined cytotoxicity of ZnO NPs, CPP and VC in GES-1 cells for abundant experiments by changing the sequence of addition of the three additives.

From the data presented in Fig. 2c and d, the cell count and the cell viability were the highest after treatment with ZnO plus CPP for 24 h. The group having the second highest cell count and cell viability was the group with CPP plus VC for 24 h. There was a small decrease in the group with CPP plus VC, compared with the group of ZnO plus CPP and the control. The CPP plus VC group had slight damage to the GES-1 cells and the ZnO plus CPP group had no toxicity toward the GES-1 cells. After treatment with the two groups mentioned above for the first 12 h, the third material was added over the second 12 h period, and the
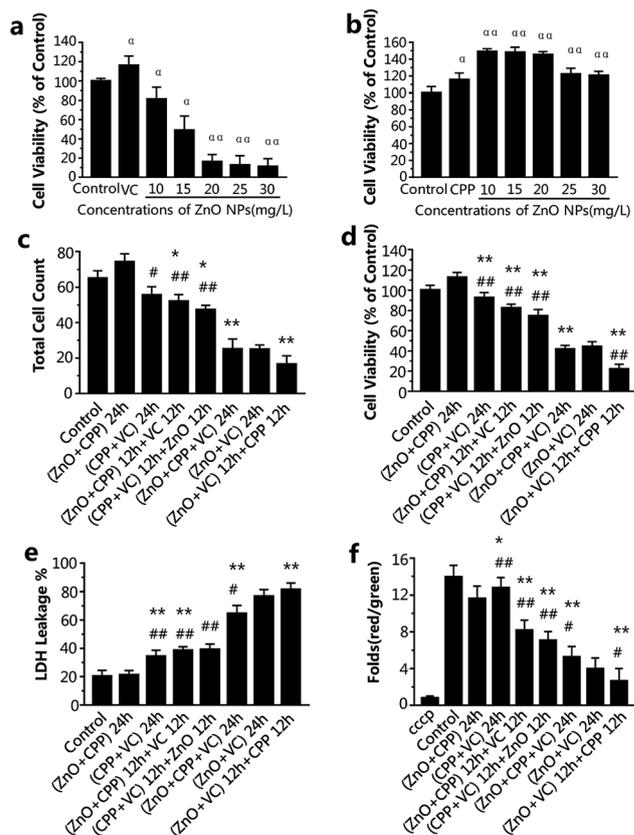
Fig. 2 Cytotoxicity evaluation after treatment with the different combined groups of ZnO NPs, CPP and VC for 24 h. (a) Cell viability analysis after incubation with VC (300 mg L^{-1}) and different concentrations (mg L^{-1}) of ZnO NPs. (b) Cell viability analysis after incubation with CPP (500 mg L^{-1}) and different concentrations (mg L^{-1}) of ZnO NPs. (c) Cell counts, (d) cell viability analysis, (e) the effects on LDH release, (f) changes in $\Delta\psi_m$ of cells in electric pulses (cells were treated with cccp ($C_9H_5ClN_4$) as the positive control). Data are presented as the mean $\pm$ S.D. $^{\alpha}P < 0.05$ compared with the control group. $^{\alpha\alpha}P < 0.01$ compared with the control group. $^*P < 0.05$ compared with the ZnO NPs plus CPP group. $^{**}P < 0.01$ compared with the ZnO NPs plus CPP group. $^{\#}p < 0.05$ compared with the ZnO NPs plus VC group. $^{\#\#}p < 0.01$ compared with the ZnO NPs plus VC group.

cell number and the cell viability continued to decrease. For the cells treated with the ZnO plus CPP group for the first 12 h, followed by the addition of VC for the second 12 h, the cell number and the viability were about 52×10^4 and 82%, respectively. The cell number and the cell viability were about 47×10^4 and 75%, respectively, for the cells first treated with the CPP plus VC group for 12 h, followed by ZnO for the other 12 h. The cell count and the cell viability after treatment with the ZnO plus VC group for the first 12 h, followed by the addition of CPP for the other 12 h, decreased to about 16×10^4 and 22%, respectively, which are lower than those treated with the ZnO plus VC group for 24 h, suggesting that significant cell death was induced by the group involving treatment with ZnO plus VC for the first 12 h, followed by the addition of CPP for the other 12 h. The cell count and the cell viability of the group treated with ZnO plus CPP plus VC for 24 h are similar to those of the group of ZnO plus VC for 24 h, indicating that CPP can protect cells from damage induced by ZnO NPs and VC.

LDH release is the result of cell apoptosis deregulation and mitochondrial machinery, which are based on the theory of intracellular enzymes releasing cells through damaged cell membranes.[20] From Fig. 2e, the LDH released from GES-1 cells incubated with ZnO plus CPP for 24 h is almost equal to that of the control group. The LDH released from cells treated with CPP plus VC for 24 h increased to about 34%. In addition, the LDH released from cells treated with the ZnO plus CPP group for the first 12 h then the addition of VC for the other 12 h was similar to that of the CPP plus VC group for the first 12 h, followed by the addition of ZnO for the other 12 h, whose LDH release percentages were about 38% and 39%, respectively. The three groups, namely cells treated with ZnO plus CPP plus VC for 24 h, ZnO plus VC for 24 h, and cells treated with ZnO plus VC for the first 12 h followed by the addition of CPP in the second 12 h (the ranking is in the order of increasing LDH release) had the greatest increase in the release of LDH from cells. It was in these groups that the cell survival rate obviously decreased. The results in Fig. 2c–e indicate that the cell membranes were badly damaged and considerable cell apoptosis occurred, which significantly and directly affected the cell viability.

The decrease in the mitochondrial membrane potential ($\Delta\psi_m$) is considered as a sign of the cell apoptotic process.[21] To investigate the changes in $\Delta\psi_m$, GES-1 cells were stained using a mitochondrial membrane potential assay kit with JC-1, which is a probe for detecting the $\Delta\psi_m$. It can form polymer J-aggregates and emit red fluorescence under high $\Delta\psi_m$. On the other hand, it keeps the monomer shape and emits green fluorescence under low $\Delta\psi_m$. Therefore, the red fluorescence/green fluorescence can be the result of the changes in $\Delta\psi_m$.[22] cccp ($C_9H_5ClN_4$) is a kind of H$^+$ ionophore that makes the inner mitochondrial membrane generate permeability, which causes the loss of the membrane potential and the apoptosis of cells; therefore, cells were treated with cccp as the positive control. The changes in $\Delta\psi_m$ in cells treated with ZnO plus CPP and CPP plus VC were almost the same as the control. The values of $\Delta\psi_m$ in other groups were dramatically decreased (Fig. 2f). Combined with the results shown in Fig. 2c–e, cells treated with ZnO plus CPP and CPP plus VC for 24 h grew well, indicating that there was almost no apoptosis when ZnO plus CPP and CPP plus VC were added over 12 h. However, during the other 12 h after adding the third material, toxicity to cells was induced. The value of $\Delta\psi_m$ in the two groups was reduced by about 7–8 times. The value of $\Delta\psi_m$ in cells treated with ZnO plus CPP and VC for 24 h, ZnO plus VC for 24 h, ZnO plus VC for 12 h and CPP for the other 12 h were the three lowest groups, whose changing trends were similar to the cell viability analysis results.

In order to study whether the incubation time had an effect on the combined cytotoxicity induced by the three additives with different adding sequences, we also chose 2 h and 6 h to do the experiment. From Fig. 3a and b, IC$_{50}$ of ZnO NPs treatment for 6 h was about 120-130 mg L^{-1}. However, the cell viabilities on exposure to different concentrations of ZnO NPs for 2 h were all higher than that of the control group (Fig. S2†), suggesting there was no toxicity to cells treated with ZnO NPs at concentrations ranging from 150 to 230 mg L^{-1} for 2 h. In consideration of the practicability of the ZnO NPs concentration,
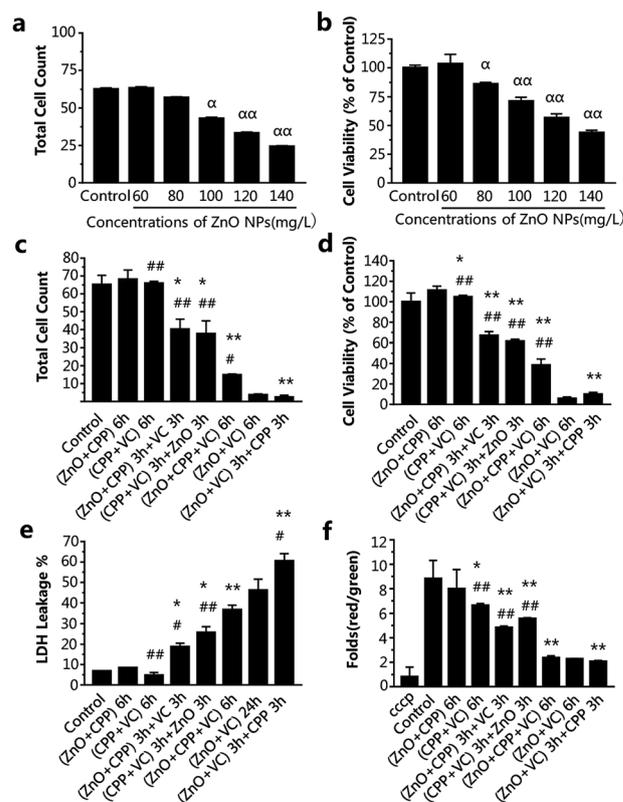

Fig. 3 Cytotoxicity evaluation after treatment with the different combined groups of ZnO NPs, CPP and VC for 6 h. (a) Cell counts after being treated with different concentrations (mg L^{-1}) of ZnO NPs. (b) Cell viability analysis after treatment with different concentrations (mg L^{-1}) of ZnO NPs. (c) Cell counts after treatment with different combined groups. (d) Cell viability analysis after treatment with different combined groups; (e) the effects on LDH release; (f) changes in $\Delta\psi_m$ of cells in electric pulses (cells are treated with cccp ($C_9H_5ClN_4$) as the positive control). Data are presented as the mean ± S.D. $^{\alpha}P < 0.05$ compared with the control group, $^{\alpha\alpha}P<0.01$ compared with the control group. $*P < 0.05$ compared with the group of ZnO NPs plus CPP. $**P < 0.01$ compared with the group of ZnO NPs plus CPP. $^{\#}p < 0.05$ compared with the group of ZnO NPs plus VC. $^{\#\#}p < 0.01$ compared with the group of ZnO NPs plus VC.

120 mg L^{-1} of ZnO NPs for 6 h, accompanied by 500 mg L^{-1} CPP and 300 mg L^{-1} VC were chosen for the experiments.

The data in Fig. 3c–f show the changes in the combined effect on GES-1 cells induced by ZnO NPs, CPP and VC with the different addition sequences for 6 h, including cytotoxicity and oxidative stress. The trend of the combined toxic effect for 6 h has been indicated to be similar to that for 24 h. The biggest difference between 24 h and 6 h is that there was no toxicity toward cells after treatment with the CPP plus VC group for 6 h, while there was low toxicity toward cells for 24 h (Fig. 2 and 3); therefore, the two nontoxic groups for 6 h are the ZnO plus CPP and CPP plus VC. It was further confirmed that VC and ZnO NPs played the key role in the combined toxicity effect. When the cells were treated with the ZnO plus CPP and CPP plus VC groups for the first half of the session, the third material (VC or ZnO NPs) was added for the second half of the session and the cell count and viability decreased to about 30–40 × 10^4 and 50–65%, respectively. The LDH release and changes in $\Delta\psi_m$

simultaneously showed corresponding changes, to a certain degree (Fig. 3c–f). When ZnO plus CPP plus VC were co-incubated in cells for 6 h, the cell viability decreased sharply. However, the survival cells were still more than four times those of cells treated with ZnO plus VC. The cell viabilities of the two groups were 38% and 5%, respectively (Fig. 3c and d). The LDH release and changes in $\Delta\psi_m$ of the cells also indicated that the injury to the membrane and the cell apoptosis of the ZnO plus CPP plus VC group were not as serious as that induced by ZnO plus VC (Fig. 3e and f). Combined with the results shown in Fig. 3, the greatest toxicity occurred with the cells that were firstly treated with ZnO plus VC for 3 h, then followed by CPP for the other 3 h. The combined toxic effect on the GES-1 cells was the same as that for 24 h. One small difference in complex cytotoxicity between 24 h and 6 h is that the cell viability after treatment with ZnO plus CPP plus VC for 6 h was obviously higher than that with ZnO plus VC, while the cell viability was similar for these two groups after being treated for 24 h (Fig. 2 and 3). The results indicate that CPP has little power to inhibit the cytotoxicity induced by ZnO plus VC when the three materials are co-incubated together in GES-1. CPP is not able to play the cytoprotective role in the presence of ZnO NPs and VC. Over a long duration, it is VC that still has the strong effect on GES-1 cells as long as the ZnO NPs are co-existent.

Intracellular redox status

Intracellular reactive oxygen species and malondialdehyde. It has been reported that cytotoxicity induced in cells by metal oxide nanoparticles is related to the oxidative stress generated by those nanoparticles.[23–27] In order to determine the combined toxicity induced concomitantly with the oxidative stress, we studied the generation of ROS and levels of MDA. High ROS generation shows that cells have oxidative damage. From Fig. 5a and b, the ROS generation and the concentration of MDA of the ZnO plus CPP group are almost equal to the control cells, while that of the ZnO plus VC group increase significantly. This shows that the cells treated with the groups without VC or ZnO for the first 12 h have the slightly higher ROS generation and MDA concentration. On the other hand, the ROS generation and the concentration of MDA of the two groups treated with ZnO and VC for 24 h increase notably whether CPP is added or not. Similar trends were observed in the short incubation time of 6 h (Fig. S3†).

Intracellular glutathione and superoxide dismutase. GSH is an abundant antioxidant that exists commonly in almost all types of cells.[28] Studies have reported that oxidative stress in cells could change the levels of GSH in cells.[29] SOD is also one of the important antioxidant enzymes in mammalian cells. After 24 h or 6 h co-incubation with ZnO plus CPP, the GSH concentration and SOD activity were almost equal to those of the control group. However, the GSH concentration and SOD activity of cells treated with the ZnO plus VC group decreased significantly (Fig. 4c, d and S3c, d†). In this respect, the cells treated first with the ZnO plus VC group with CPP added later resemble the ZnO plus VC group. The GSH concentration and SOD activity of that group decreased in a similar manner to that
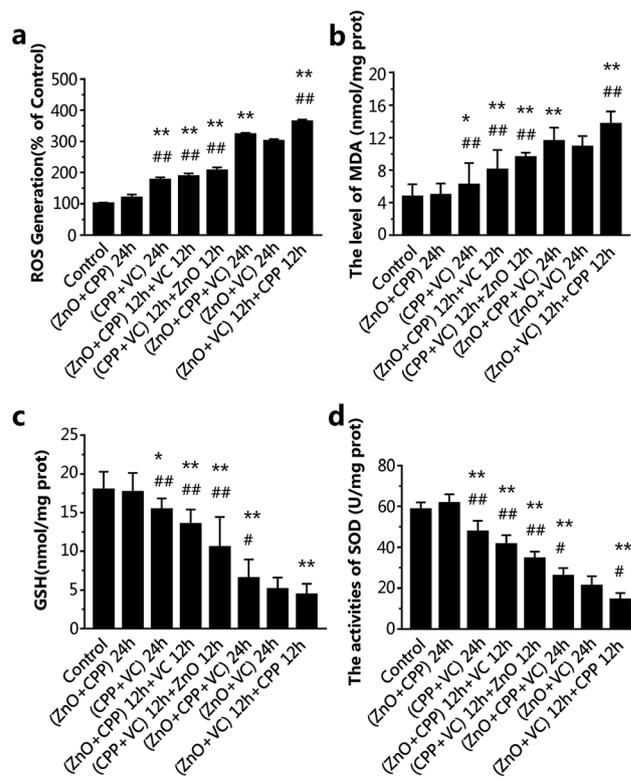

Fig. 4 Intracellular redox production after incubation with ZnO NPs, CPP and VC in different systems for 24 h. (a) ROS generation; (b) MDA concentration; (c) GSH concentration; (d) SOD activity. Data are presented as the mean ± S.D. *$P < 0.05$ compared with the group of ZnO NPs plus CPP. **$P < 0.01$ compared with the group pf ZnO NPs plus CPP. #$p < 0.05$ compared with the group of ZnO NPs plus VC. ##$p < 0.01$ compared with the group of ZnO NPs plus VC.

of the ZnO plus VC group. The GSH concentration and SOD activity of the ZnO plus CPP plus VC group decreased to nearly half of the ZnO plus CPP group but were still higher than that of the ZnO plus VC group. The GSH and SOD activity of the other two groups (firstly adding ZnO plus CPP then VC and CPP plus VC then ZnO) were significantly reduced as compared to the ZnO plus CPP group. The GSH concentration and SOD activity of the cells treated with CPP plus VC were all lower than the control cells (Fig. 4c and d) but for 6 h, they were slightly higher than the control cells (Fig. S3c and d). This indicates that uniting CPP with VC for a short time (6 h) can protect cells against oxidative damage; however, the reverse will occur over time such as after 24 h.

DNA fluorescence staining

Cell death can be determined by cell nuclear size and roundness, which are among the general cell morphological changes indicating cell apoptosis.[30] We further observed cell morphological changes to investigate the effects induced on GES-1 cells by the three materials. Fig. 5a and b show that most of the cells treated with ZnO plus CPP for 24 h have the normal spindle as the normal cellular morphology. The cells shrank and there were morphological changes in the different levels of the other groups (Fig. 5c–h). There was an obvious loss of cell membrane
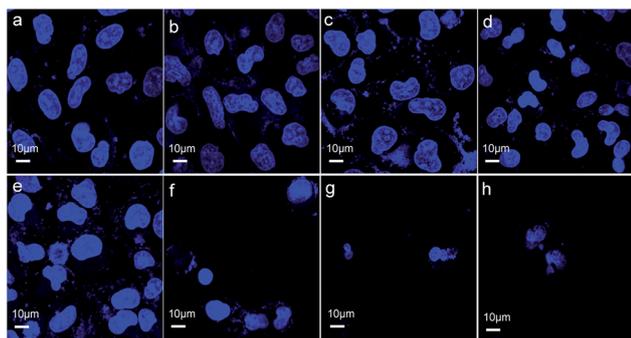
Fig. 5 Observations of the morphological changes in GES-1 after co-incubation in 15 mg L^{-1} of ZnO NPs, 500 mg L^{-1} of CPP, 300 mg L^{-1} of VC with different combination groups for 24 h. (a) The control cells stained by DAPI; (b) the cells treated with (ZnO + CPP) for 24 h and stained by DAPI; (c) the cells treated with (CPP + VC) for 24 h and stained by DAPI; (d) the cells treated with (ZnO + CPP) for 12 h + VC for 12 h and stained by DAPI; (e) the cells treated with (CPP + VC) for 12 h + ZnO for 12 h and stained by DAPI; (f) the cells treated with (ZnO + CPP + VC) for 24 h and stained by DAPI; (g) the cells treated with (ZnO + VC) for 24 h and stained by DAPI; (h) the cells treated with (ZnO + VC) for 12 h + CPP for 12 h and stained by DAPI.

integrity and the cell count sharply declined after treatment with the three groups: ZnO plus CPP plus VC; ZnO plus VC for 24 h; ZnO plus VC for 12 h then CPP added for the other 12 h. The changes in the GES-1 cell morphology after being treated with the complex systems for 6 h were consistent with the results for 24 h. Cells treated with ZnO plus CPP and CPP plus VC grew well (Fig. S4a–c†). Except for the three groups mentioned above, cells treated with the other combined groups were shrunken and rounded. The cell membranes lost integrity and the nuclei condensed (Fig. S4d–h†). These results further demonstrated that CPP cannot prevent the cytotoxicity induced by ZnO NPs plus VC. CPP has little cytoprotective effects on GES-1 cells induced by ZnO NPs in the presence of VC.

Mechanistic study of the combined cytotoxicity effects

The dissociated and solubilized Zn ions are the main contributors to the toxicity to cells caused by ZnO NPs because Zn ions damage cellular zinc homeostasis as a result of lysosomal and mitochondrial damage, even leading to cell death.[31–33] Ivask et al. reported that Zn^{2+} released from nanoparticles contributed to the cytotoxicity of ZnO NPs.[34] Wang et al. found that O-MWCNTs enter into C17.2 cells and Hela cells easily with the Zn ions absorption onto O-MWCNTs and bring more Zn^{2+} into the cells, thus inducing more serious cytotoxicity.[35] It has been demonstrated that CPP can prevent the sedimentation of calcium ions, such as with calcium phosphate.[36,37] Our previous study confirmed that VC promoted the ZnO NPs endocytosis process, leading to the increasing concentration of Zn^{2+} in GES-1 cells.[8] We tested the cell viability of GES-1 cells treated with ZnCl$_2$ solution. There is a one-to-one correspondence between the concentration of ZnCl$_2$ and ZnO NPs at the same incubation time. In Fig S1a and S5a,† the cell viability caused by ZnCl$_2$ is lower compared to ZnO NPs of the corresponding concentrations, as well as what was shown in Fig. S5b† and 3b for 6 h.

Compared with Fig. S1a, S5† and 3b, it is obvious that the cytotoxicity of Zn^{2+} is stronger than ZnO NPs. Furthermore, we quantified the dissolution of Zn^{2+} from ZnO NPs in high-glucose DMEM with 10% fetal bovine serum in composite systems. The fewest dissolved zinc ions originated from the ZnO NPs in the group of ZnO plus CPP at 24 h or 6 h (Fig. 6). The amounts of Zn ions in the other five groups gradually increased. The amount of Zn ions was the highest in the group with ZnO plus VC in the first period followed by mixing in CPP, which was over two times that in the group of ZnO plus CPP. Harzer found that zinc did not bind to casein at pH 2 and zinc dephosphorylated casein at pH 7.4.[38] Wang et al. demonstrated that the phosphorylation of the CPP is the key role of Zn binding by α-casein. The phosphorylation of a peptide significantly enhances Zn binding.[39] Zn ions in the ZnO plus CPP group were the lowest when compared with other groups. It was demonstrated that the acidity of VC can promote Zn ion concentration from ZnO NPs.[8]

From the results shown in Fig. 2, 3 and 6, it can be concluded that the dissolution of Zn^{2+} from ZnO NPs in different systems is proportional to the cytotoxicity induced by the corresponding systems, adjusted for both test times of 24 h and 6 h. CPP has the weak power to control the ZnO dissolution induced by VC when the three materials co-exist.

To confirm that the concentration of Zn ions plays a key role in inducing the combined toxicity, we analysed the concentration of zinc ions in GES-1 cells. TSQ is a common Zn ions sensor. Zn^{2+} binding can be accompanied by an intense fluorescence emission spectrum. TSQ uses its related fluorophores to mark the Zn ions.[40] From Fig. 7, the control cells and cells treated with CPP plus VC have few blue fluorophores. The blue fluorophores of the Zn ions were slightly increased for the cells treated with the three groups, namely, ZnO NPs plus CPP only, firstly adding ZnO plus CPP then adding VC, and firstly adding CPP plus VC then adding ZnO NPs (Fig. 7b, d and e). However, cells treated with the other groups of ZnO plus CPP plus VC,
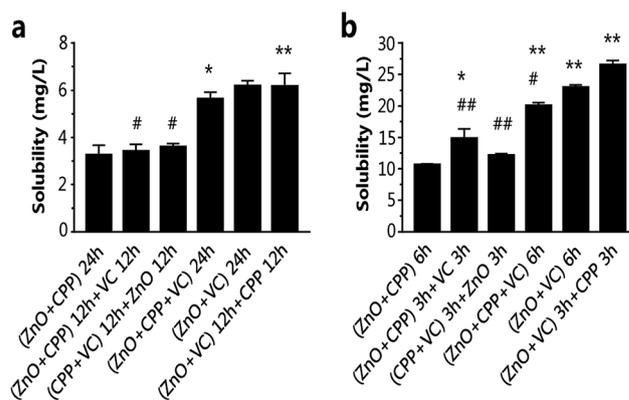

Fig. 6 Solubility of ZnO NPs in different systems at different time. (a) Solubility of 15 mg L^{-1} ZnO NPs at 24 h; (b) solubility of 120 mg L^{-1} ZnO NPs at 6 h. Data are presented as the mean ± S.D. *$P < 0.05$ compared with the group of ZnO NPs plus CPP. **$P < 0.01$ compared with the group of ZnO NPs plus CPP. #$p < 0.05$ compared with the group of ZnO NPs plus VC. ##$p < 0.01$ compared with the group pf ZnO NPs plus VC.
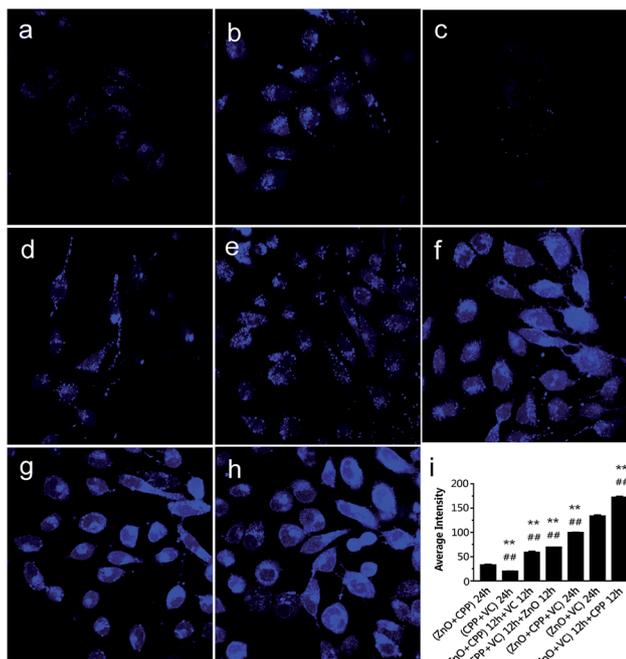
Fig. 7 The density of zinc ions in GES-1 cells after co-incubation with 15 mg L^{-1} of ZnO NPs, 500 mg L^{-1} of CPP, 300 mg L^{-1} of VC with different systems for 24 h. The cells were stained with TSQ. (a) The control cells; (b) the cells treated with (ZnO + CPP) for 24 h; (c) the cells treated with (CPP + VC) for 24 h; (d) the cells treated with (ZnO + CPP) for 12 h + VC for 12 h; (e) the cells treated with (CPP + VC) for 12 h + ZnO for 12 h; (f) the cells treated with (ZnO + CPP + VC) for 24 h; (g) the cells treated with (ZnO + VC) for 24 h; (h) the cells treated with (ZnO + VC) for 12 h + CPP for 12 h. (i) Analysis of the average fluo-rescence intensity of zinc ions in GES-1 cells after incubation with different groups for 24 h. **P < 0.01 compared with the ZnO NPs plus CPP group, $^{##}p$ < 0.01 compared with the ZnO NPs plus VC group.

ZnO NPs plus VC only, and firstly adding ZnO NPs plus VC then adding CPP presented very powerful blue fluorophores of Zn ions (Fig. 7f–h). At the same time, the cell morphology also changed by different degrees. Similar changes happened in the 6 h co-incubation groups (Fig. S6†). The average intensity of each group is shown in Fig. 7i and S5i.† The average intensity of cells treated with ZnO NPs plus CPP was 32 for 24 h and 26 for 6 h, ZnO NPs plus VC was 133 for 24 h and 113 for 6 h. The most toxic group was up to 172 for 24 h and 134 for 6 h and the average intensity of cells treated with other toxic groups also increased to different degrees. Based on the results shown in Fig. 6, 7 and S6,† we concluded that the concentration of dis-solved Zn ions was the main factor for determining the toxicity of combined systems of ZnO NPs with VC and CPP.

Zn absorption in the small intestines

The results mentioned above have demonstrated that the amount of Zn ions is the key factor in inducing the cytotoxicity of ZnO NPs, CPP and VC. It verified that CPP increased the amount of soluble calcium in the intestinal lumen, increasing the mineral absorption in the small intestine.[41–43] Seal et al. found that the colonic tissue from +pectin rats was where the highest section of the small intestine was transferred Zn.[16] Y. Li

et al. demonstrated that CPP can directly affect the function of the intestinal mucosa in vitro to promote the calcium; it can only bind calcium in the lumen of the intestine.[44] The intestines are among the most important tissues in the digestion and metabolism of nutrients. In order to understand the absorption of different composite groups, we used the everted gut sacs model to investigate the Zn absorption of different combined groups in the intestine. The Zn absorption on sacs in different groups are shown in Fig. 8a. The amounts of Zn^{2+} in different groups were gradually increased. Zn ions remained the fewest in sacs in the ZnO plus CPP group only. On the contrary, the amounts of Zn^{2+} increased fiercely in the ZnO plus VC group, which were 13.8 µg and 57.0 µg, respectively. The amount of Zn^{2+} was up to 59.5 µg in the group with ZnO plus VC followed by the addition of CPP. There are some Zn ions that can go through the intestinal sacs, which means that the Zn ions were metabolised in the everted gut sac model (Fig. 8b). The dis-solved Zn^{2+} absorption of ZnO NPs in the small intestine was influenced by CPP and VC with different sequences of addition.

In this study, we used the cell model to research the combined effects on GES-1 cells of ZnO NPs, CPP and VC, as well as the method of the everted gut sac to explore Zn^{2+} absorption in the small intestines in different systems of ZnO NPs, CPP and VC. The whole process is shown in Fig. S7.† The study focuses on the combined effect and its mechanism on GES-1 cells treated with ZnO NPs, CPP and VC of varied incu-bation times, as well as Zn^{2+} absorption in the small intestine. We determined that the toxicity is different with the different sequences of addition of the three materials. Zn^{2+} amounts dissolved from ZnO NPs changed in different combined systems and are the key factors in determining the toxicity of the combined system of ZnO NPs, VC and CPP. CPP shows the very weak protective function to GES-1 cells, induced by ZnO plus VC. When CPP was later added to the group of ZnO plus VC, CPP
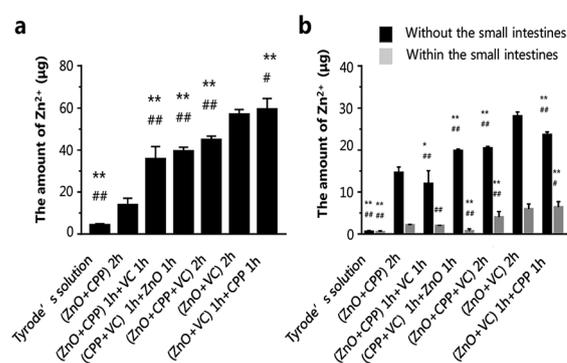

Fig. 8 The zinc ions absorption of the small intestines. (a) The amount of zinc ions absorption on small intestines after co-incubation with different systems for 2 h; (b) the amount of zinc ions after co-incu-bation with different systems with small intestines for 2 h (black column: the amount of zinc ions in the solutions without the small intestines; gray column: the amount of zinc ions in the solutions within the small intestines). Data are presented as the mean ± S.D. *P < 0.05 compared with the group of ZnO NPs plus CPP. **P < 0.01 compared with the group of ZnO NPs plus CPP. $^{#}p$ < 0.05 compared with the group of ZnO NPs plus VC. $^{##}p$ < 0.01 compared with the group of ZnO NPs plus VC.

could even promote the cytotoxicity and generate more Zn ions dissolved from ZnO NPs. The acidity of VC always plays a leading role in controlling the Zn ion amounts dissolved from ZnO NPs in the complex groups with three materials. Furthermore, Zn absorption in the small intestines also changes with different addition sequences for the additives.

Experimental section

Materials

Food grade ZnO NPs were obtained from Wuxi Zehui Chemical Industry Co. Ltd. (Jiangsu, China). CPP was obtained from Beijing Weier Healthy Food Co. Ltd. (Beijing, China). Vitamin C was purchased from Guangzhou Yuanchang Commercial Co. Ltd. (Guangdong, China).

Characterization of ZnO NPs

The morphology and size of ZnO NPs were observed by TEM (JEM-200CX, JEOL, Japan). The crystalline phase of ZnO NPs was analysed by XRD (Rigaku Co., Tokyo, Japan). The zeta potential and the hydrodynamic size of ZnO NPs with different systems in water and culture medium were tested on a Nanosizer (Zetasizer 3000 HS, Malvern, UK). The concentration of ZnO NPs was adjusted to 0.01% in each system at mass fraction.

Cell culture

GES-1 cells, human gastric epithelium cells, were bought from the Chinese Academy of Sciences. Dulbecco's Modified Eagle's Medium (DMEM) and fetal bovine serum were obtained from Gino Biological Pharmaceutical Technology Co. Ltd. (Hangzhou, China). Cells were cultured to confluence and supplied with high-glucose DMEM and 10% FBS in 25 cm^2 flasks and incubated in a humidified incubator with 5% CO_2 and 95% air at 37 °C. GES-1 cells used in all assays were 80% confluent in each flask.

Cell proliferation

Cell viability assays were performed using a CCK-8 Kit (Dojindo Laboratories, Japan) following the manufacturer's instructions. The cell viability is shown as the percentage of viable cells contained in the total cells. Briefly, 4×10^3 cells (test time 24 h) or 6×10^3 cells (test time 6 h) per well, with 100 μL medium, were cultured in 96-well plates and pre-incubated for 24 h at 37 °C and 5% CO_2 atmosphere. The original 100 μL medium was then replaced with new medium containing different concentrations of $ZnCl_2$, ZnO NPs, CPP, VC respectively and two or three materials were combined for an additional 24 h or 6 h. The cell viability of each well was determined with the CCK-8 kit by following the instruction manual, and the absorbance of each well at 450 nm was detected on a microplate reader (Thermo, USA).

Cell count

Cell counts were determined using a hemocytometer (Shanghai Qiujing Biochemical reagent and Instrument Co., Ltd, China).

Briefly, GES-1 cells were seeded in six-well plates (1.5×10^5 cells per well for a test time of 24 h, or 2.5×10^5 cells per well for a test time of 6 h), then after a 24 h attachment period, the cells were incubated in different mixed media of ZnO NPs & CPP & VC with different test times. The attached cells were then trypsinized with 25% trypsin–EDTA (GIBCO, Invitrogen, USA) and counted using a hemocytometer.

Cell membrane integrity

The release of the cytosolic enzyme lactate dehydrogenase (LDH) into the culture was detected to assess cell death by testing cellular membrane damage. Data were expressed as percent viability of cells based on LDH released from positive control cells.[45] It was determined by using a commercially available kit (Beyotime Laboratories, China). Briefly, GES-1 cells were seeded in 96-well plates (4×10^3 cells per well for test time of 24 h, or 6×10^3 cells per well for a test time of 6 h). After a 24 h attachment period, cells were treated in different mixed media of ZnO NPs and CPP and VC with different orders for the test times. The positive control cells were treated with cell lysis buffer for 1 h before centrifugation (400 g, 5 min). The supernatant was shifted to a new 96-well plate, adding 60 μL of LDH work solution for 30 min. The LDH of each well was measured at 490 nm using a microplate reader (Thermo, USA).

Mitochondrial transmembrane potential ($\Delta\psi_m$) determination

Briefly, GES-1 cells (1.5×10^5 cells per well for 24 h or 2.5×10^5 cells per well for 6 h) were seeded in six-well plates. After a 24 h growth time, cells were treated in different mixed materials. After the test time (24 h or 6 h), cells were harvested and treated with a mitochondrial membrane potential assay kit with JC-1 (Beyotime Laboratories, China). The fluorescent lipophilic probe JC-1 was loaded at 37 °C for 20 min and then washed with JC-1 buffer solution ($1\times$) twice. The fluorescence of JC-1 forms was detected by a microplate reader (Thermo, USA).

Measurement of reactive oxygen species and malondialdehyde

ROS were measured using a Reactive Oxygen Species Assay kit (Beyotime Laboratories, China). It used the oxidation-sensitive fluorophore $2'7'$-dichlorofluorescein diacetate (DCFH-DA), a non-fluorescent compound, to freely pass through the cells and was hydrolyzed by esterases to $2',7'$-dichlorofluorescein (DCFH). It indicated the level of intracellular ROS by the way in which DCFH was oxidized to the fluorescent $2',7'$-dichlorofluorescein (DCF) in the presence of peroxides. Briefly, cells treated with ZnO NPs & CPP & VC were harvested and incubated with 20 μmol L^{-1} DCFH-DA dissolved in FBS-free medium at 37 °C for 20 min, and were then washed three times with FBS-free medium. Cellular fluorescence was quantified by a microplate reader (Thermo, USA) at 525 nm emission wavelength. Intracellular ROS production was expressed as a percentage of control cells.

Malondialdehyde (MDA) is a natural product of biological lipid oxidation and a common membrane lipid peroxide index.

MDA was analysed using an assay kit (Jiancheng Bioengineering Institute, China). Briefly, cells were harvested by trypsinization and were prepared by ultrasonication (Vcx-130 PB, Sonics Corp., USA) with extracting solution to obtain cellular extracts. The assay was then carried out based on the manufacturer's instructions for the MDA assay kit. The same method was used for cell-breaking and protein concentration was determined with the enhanced BCA Protein Assay Kit (Beyotime Laboratories, China). A microplate reader (Thermo, USA) at a wavelength of 530 nm was used to measure the concentration of MDA, which can react with thiobarbituric acid (TBA) to produce a stable red compound. MDA levels were expressed as nmol per mg protein.

Measurement of glutathione and superoxide dismutase

GSH is a natural antioxidant in cells. However, as a result of free radical scavenging or the reduction of peroxides, the level of GSH is reduced.[46] The concentration of GSH was determined by an assay kit (Jiancheng Bioengineering Institute, China) and measured using a microplate reader (Thermo, USA) at a wavelength of 405 nm. All procedures were according to the manufacturer's instructions.

SOD is a significant enzyme in mammalian cells, which has the ability to inhibit the oxidation of O^{2-} produced in the xanthine/xanthine oxidase system. The activity of SOD was analysed by an assay kit (Jiancheng Bioengineering Institute, China) and measured using a microplate reader (Thermo, USA) at a wavelength of 450 nm. All procedures were according to the manufacturer's instructions.

DNA fluorescent staining and confocal laser scanning microscopy studies

The fluorescence probe 4,6-diamidino-2-phenylindole (DAPI) is a popular nuclear counterstain in multicolor fluorescence techniques. It stains nuclei specifically, with little or no cytoplasm labeling.[47] Briefly, GES-1 cells were pre-cultured in culture medium containing ZnO NPs plus CPP, CPP plus VC, ZnO NPs plus VC, CPP plus VC and ZnO NPs plus CPP plus VC with different orders, respectively for 6 h or 24 h. The cells were washed with D-Hanks and DAPI work solutions. The cells were kept in a 2 mg L^{-1} DAPI work solution for 15 min in the dark at 37 °C. The cells were washed twice with methanol to remove excess DAPI and were detected under a confocal microscope (Occult International Ltd., Germany) with an excitation wavelength of 405 nm.

Fluorescence assessment of zinc ions and cell morphology

A commonly used Zn^{2+} fluorophore is 6-methoxy-8-p-toluenesulfonamidoquinoline (TSQ) (Shanghai Meilian Biotechnology Co. Ltd., China). A method developed by Meeusen for this assay was used.[40] Briefly, GES-1 cells were pre-cultured in culture medium containing ZnO NPs plus CPP, CPP plus VC, ZnO NPs plus VC, CPP plus VC and ZnO NPs plus CPP plus VC with different orders respectively for 6 or 24 h. The cells were washed three times by D-Hanks. The cells were stained for 30 min using a solution of 10 mg L^{-1} TSQ in D-Hanks in a dark incubator.

Finally, the stained cells were washed three times with D-Hanks to remove excess dye and detected under a confocal microscope (Occult International Ltd., Germany) with an excitation wavelength of 405 nm. Then, we used confocal microscopy to determine the average fluorescence intensity of Zn^{2+} in GES-1 cells.

Zinc content analysis

Each pure solution (2 mL) was prepared with high-glucose DMEM and 10% FBS containing a mixture of ZnO NPs and CPP and VC and then allowed to stand at 37 °C for the test time (24 h or 6 h). After the test time, the solutions were centrifuged at 10 000 rpm for 20 min to remove the undissolved powder. Clear solutions were collected, digested and analyzed for zinc content. The digestion was first performed in aqua regia (nitric acid : hydrochloric acid = 1 : 3 v/v) overnight for complete digestion. The mixed solutions were then heated at about 150 °C to remove the remaining acid until the solutions became colorless. The solutions were then transferred and diluted to 3 mL with ultrapure water and the zinc concentration in the digested samples was detected by inductively coupled plasma atomic emission spectrometry (ICP-AES, Leeman Labs., USA).

Zn^{2+} absorption studies in small intestine sacs

Animals and treatments. Ten male Kunming mice (25 ± 2 g) were purchased from the Slack Experimental Animal Center (Shanghai, China). All animals were housed in groups of 5 in plastic cages with a stainless steel mesh lid in a ventilated animal room. Room temperature was maintained at 20 ± 2 °C, relative humidity at 60 ± 10%, and there was a 12 h light–dark cycle. Distilled water and aseptic food for mice were available *ad libitum*. The animals were acclimated to this environment for one week before the experiment. All animal procedures were performed in accordance with the Guidelines for the Care and Use of Laboratory Animals of Shanghai University, and experiments were approved by the Animal Ethics Committee of Shanghai University.

We used the everted gut sac method for this experiment, which was performed as previously outlined.[48] Briefly, the ten male mice were fasted overnight (free access to water) and were sacrificed by cervical dislocation and exsanguination; the small intestines were removed and washed three times with Tyrode's solution at room temperature. The intestines were immediately placed in oxygenated (O_2/CO_2, 95%:5%) medium at 37 °C, then were everted on a puncture needle (0.8 mm in diameter) and were cut into several sections to make sacs. One end was clamped before filling with 200 μL Tyrode's solution using a 1 mL plastic syringe. Small sacs (5 cm in length each) were then tied using silk braided sutures. Each sac was placed in a 6-well plate (one sac per well) containing 3 mL of different solutions (ZnO NPs, CPP, VC and their systems in different orders) with Tyrode's solution. Finally, the resulting gut sacs were incubated at 37 °C in a humidified incubator with 5% CO_2 and 95% air at 37 °C for 2 h. At the appropriate time points, the sacs were removed and washed four times in Tyrode's solution. The sacs were cut open and the contents were drained into small

tubes. The solutions (3 mL) and each sac were also collected in other small tubes, respectively. The collected solutions were all centrifuged to remove undissolved ZnO NPs powder and then all the samples including solutions and sacs mentioned above were digested for zinc content analysis. The digestion was first performed in aqua regia (nitric acid : hydrochloric acid = 1 : 3 v/v) overnight for complete digestion, and to the sac samples were added 1 mL of H_2O_2 after aqua regia. The samples were all heated at about 150 °C to remove the remaining acids until the solutions were colorless and clear. At last, the solutions were transferred and diluted to 3 mL. The zinc concentration in the digested samples was detected by inductively coupled plasma atomic emission spectrometry (ICP-AES, Leeman Labs., USA).

Tyrode's solution was composed of two kinds of solutions: one is NaCl 8.0 g, KCl 0.28 g, $NaHCO_3$ 1.0 g, NaH_2PO_4 0.05 g, $MgCl_2$ 0.1 g in 500 mL of ultrapure water; the other solution is $CaCl_2$ 0.2 g in 500 mL of ultrapure water. Glucose was added (1.0 g) to the two kinds of solution (v/v = 1 : 1) mentioned above by stirring. They were then placed in an airtight freezer container before use.

Statistical analysis. Results were expressed as the mean ± standard deviation (SD). Comparisons among the groups were analysed by t-tests of one-way analysis of variance (ANOVA). A value of $p < 0.05$ was viewed as statistically significant.

Conclusions

ZnO NPs, CPP and VC are commonly used as food additives in our daily life. On the foundation of combined toxicity studies in GES-1 cells induced by ZnO NPs plus CPP and ZnO NPs plus VC, we further explored the combined effect of the three ingredients with different adding sequences. Three additives with different sequences of addition have different effects on the combined toxicity of ZnO NPs. The cytoprotective effect of CPP on GES-1 cells against the toxicity induced by ZnO NPs is very limited in the presence of VC. Zn ions absorption in the small intestines also illustrates that CPP is not able to decrease the amount of dissolved Zn^{2+} from ZnO NPs in the presence of VC. Therefore, the effect of VC is much stronger than that of CPP on the toxicity induced by ZnO NPs. When incorporating additives into food, the different adding sequences should be taken into account to bring down security risks besides safety concentrations. Our findings declare the importance of adding sequences and ingredients in the complex system of the safety of food additives.

Conflicts of interest

There are no conflicts to declare.

Acknowledgements

Notes and references

1 E. Frohlich and E. Roblegg, *Toxicology*, 2012, **291**, 10–17.
2 L.-T. Lim, *Trends Food Sci. Technol.*, 2005, **16**, 574–575.
3 B. Bao, A. S. Prasad, F. W. J. Beck, D. Snell, A. Suneja, F. H. Sarkar, N. Doshi, J. T. Fitzgerald and P. Swerdlow, *Transl. Res.*, 2008, **152**, 67–80.
4 K. H. Brown, J. M. Peerson, S. K. Baker and S. Y. Hess, *Food Nutr. Bull.*, 2009, **30**, 12–40.
5 T. Villanueva, *CMAJ*, 2011, **183**, E774.
6 N. Asare, C. Instanes, W. J. Sandberg, M. Refsnes, P. Schwarze, M. Kruszewski and G. Brunborg, *Toxicology*, 2012, **291**, 65–72.
7 M. Rossi, F. Cubadda, L. Dini, M. L. Terranova, F. Aureli, A. Sorbo and D. Passeri, *Trends Food Sci. Technol.*, 2014, **40**, 127–148.
8 Y. Wang, L. Yuan, C. Yao, L. Ding, C. Li, J. Fang, K. Sui, Y. Liu and M. Wu, *Nanoscale*, 2014, **6**, 15333–15342.
9 Y. Cao, M. Roursgaard, A. Kermanizadeh, S. Loft and P. Moller, *Int. J. Toxicol.*, 2015, **34**, 67–76.
10 S. Li, W. Song and M. Gao, *Procedia Environ. Sci.*, 2013, **18**, 100–105.
11 N. Sun, H. Wu, M. Du, Y. Tang, H. Liu, Y. Fu and B. Zhu, *Trends Food Sci. Technol.*, 2016, **58**, 140–148.
12 D. D. Kitts, *Trends Food Sci. Technol.*, 2005, **16**, 549–554.
13 E. A. Awadalla, *Exp. Toxicol. Pathol.*, 2012, **64**, 431–434.
14 Y. Wang, L. Yuan, C. Yao, L. Ding, C. Li, J. Fang and M. Wu, *RSC Adv.*, 2014, **4**, 42168–42174.
15 M. A. Alam, F. I. Al-Jenoobi and A. M. Al-Mohizea, *J. Pharm. Pharmacol.*, 2012, **64**, 326–336.
16 C. J. Seal and J. C. Mathers, *Br. J. Nutr.*, 2007, **62**, 151.
17 D. R. Elias, A. Poloukhtine, V. Popik and A. Tsourkas, *Nanomedicine*, 2013, **9**, 194–201.
18 N. Hoshyar, S. Gray, H. Han and G. Bao, *Nanomedicine*, 2016, **11**, 673–692.
19 L. Shang, K. Nienhaus and G. U. Nienhaus, *J. Nanobiotechnol.*, 2014, **12**, 5.
20 V. Jurisic, S. Radenkovic and G. Konjevic, *Adv. Exp. Med. Biol.*, 2015, **867**, 115–124.
21 W. G. Tatton and C. W. Olanow, *Biochim. Biophys. Acta, Bioenerg.*, 1999, **1410**, 195–213.
22 L. He, D. Xiao, J. Feng, C. Yao and L. Tang, *Med. Oncol.*, 2017, **34**, 24.
23 Y. Wang, L. Ding, C. Yao, C. Li, X. Xing, Y. Huang, T. Gu and M. Wu, *Sci. China Mater.*, 2017, **60**, 93–108.
24 S. Chattopadhyay, S. K. Dash, S. Tripathy, B. Das, D. Mandal, P. Pramanik and S. Roy, *Chem.-Biol. Interact.*, 2015, **226**, 58–71.
25 W. Lin, Y. Xu, C.-C. Huang, Y. Ma, K. B. Shannon, D.-R. Chen and Y.-W. Huang, *J. Nanopart. Res.*, 2008, **11**, 25–39.
26 Y. W. Huang, C. H. Wu and R. S. Aronstam, *Materials*, 2010, **3**, 4842–4859.
27 T. Mocan, S. Clichici, L. Agoston-Coldea, L. Mocan, S. Simon, I. R. Ilie, A. R. Biris and A. Muresan, *Acta Physiol. Hung.*, 2010, **97**, 247–255.

28 H. J. Gukasyan, K. J. Kim, V. H. L. Lee and R. Kannan, *Ocul. Surf.*, 2007, **5**, 269–279.

29 T. P. Dalton, Y. Chen, S. N. Schneider, D. W. Nebert and H. G. Shertzer, *Free Radical Biol. Med.*, 2004, **37**, 1511–1526.

30 B. Daniel and M. A. DeCoster, *Brain Res. Protoc.*, 2004, **13**, 144–150.

31 K. Kasemets, A. Ivask, H. C. Dubourguier and A. Kahru, *Toxicol. In Vitro*, 2009, **23**, 1116–1122.

32 M. Heinlaan, A. Ivask, I. Blinova, H. C. Dubourguier and A. Kahru, *Chemosphere*, 2008, **71**, 1308–1316.

33 M. Mortimer, K. Kasemets and A. Kahru, *Toxicology*, 2010, **269**, 182–189.

34 A. Ivask, T. Titma, M. Visnapuu, H. Vija, A. Kakinen, M. Sihtmae, S. Pokhrel, L. Madler, M. Heinlaan and V. Kisand, *Curr. Top. Med. Chem.*, 2015, **15**, 1914.

35 L. Wang, J.-H. Liu, Z.-M. Song, Y.-X. Yang, A. Cao, Y. Liu and H. Wang, *Sci. China: Chem.*, 2016, **59**, 910–917.

36 H. Meisel and C. Olieman, *Anal. Chim. Acta*, 1998, **372**, 291–297.

37 R. Berrocal, S. Chanton, M. A. Juillerat, B. Favillare, J.-C. Scherz and R. Jost, *J. Dairy Res.*, 2009, **56**, 335–341.

38 H. Kauer, *Am. J. Clin. Nutr.*, 1982, **35**, 981–987.

39 J. Wang, K. Green, G. McGibbon and B. McCarry, *Rapid Commun. Mass Spectrom.*, 2007, **21**, 1546–1554.

40 J. W. Meeusen, H. Tomasiewicz, A. Nowakowski and D. H. Petering, *Inorg. Chem.*, 2011, **50**, 7563–7573.

41 R. Sato, M. Shindo, H. Gunshin, T. Noguchi and H. Naito, *Biochim. Biophys. Acta, Protein Struct. Mol. Enzymol.*, 1991, **1077**, 413–415.

42 R. Sato, T. Noguchi and H. Naito, *J. Nutr. Sci. Vitaminol.*, 1986, **32**, 67–76.

43 Y. S. Lee, T. Noguchi and H. Naito, *Br. J. Nutr.*, 1980, **43**, 457–467.

44 Y. Li, D. Tomé and J. F. Desjeux, *Reprod., Nutr., Dev.*, 1989, **29**, 227.

45 C. McCracken, A. Zane, D. A. Knight, P. K. Dutta and W. J. Waldman, *Chem. Res. Toxicol.*, 2013, **26**, 1514–1525.

46 R. Masella, R. Di Benedetto, R. Varì, C. Filesi and C. Giovannini, *J. Nutr. Biochem.*, 2005, **16**, 577–586.

47 T. N. Siegel, D. R. Hekstra and G. A. Cross, *Mol. Biochem. Parasitol.*, 2008, **160**, 171–174.

48 X. M. Yan, C. H. Kim, C. K. Lee, J. S. Shin, I. H. Cho and U. D. Sohn, *Korean J. Physiol. Pharmacol.*, 2010, **14**, 71–75.